Oceanologia 63 (2021) 321—328

Available online at www.sciencedirect.com

ScienceDirect

journal homepage: www.journals.elsevier.com/oceanologia

ORIGINAL RESEARCH ARTICLE

Kelvin-Helmholtz instabilities in the Colorado River Delta, Gulf of California

Noel Carbajal[a,*], José Tuxpan Vargas[a], Juan Heberto Gaviño Rodríguez[b], Yovani Montaño Ley[c], David Alberto Salas de León[c]

[a] *San Luis Potosí Institute of Scientific Research and Technology, Mexico*
[b] *Centro Universitario de Investigaciones Bibliotecológicas (CUIB), University of Colima, Mexico*
[c] *Institute of the Oceano Sciences and Limnology, The National Autonomous University of Mexico, Mexico*

Received 17 December 2020; accepted 19 March 2021
Available online 1 April 2021

KEYWORDS
Kelvin-Helmholtz instabilities;
Colorado River Delta;
Tides;
Undulating topography;
Suspended sediment

Abstract In the Colorado River Delta, the interaction of tidal currents and sea-bottom sediment formed, in geological times, large-scale seabed patterns known as sandbanks. These patterns are oriented along the delta, almost parallel to the dominant tidal flow, with the bathymetry having an undulating character across the delta. Calculations and analysis showed that the interaction of tidal currents with the bathymetry causes velocity shears, faster flowing over the ridges than in the troughs. Kelvin-Helmholtz instabilities emerge from the velocity shear, and a large amount of suspended sediment makes the instabilities visible in satellite images. The physical and dynamic conditions allowed us to find an explanation for the existence of these Kelvin-Helmholtz instabilities. Since sandbanks have been observed in different seas such as the North Sea, The Gulf of Korea, the Gulf of Khambhat in India, the Jiangsu coast in China, the Persian Gulf, and Moreton Bay in Australia, the results suggest the existence of instabilities in these areas. Satellite images, intense tidal currents, undulating topography, and suspended sediment made it possible to explain the generation and identification of Kelvin-Helmholtz instabilities.

* Corresponding author at: San Luis Potosí Institute of Scientific Research and Technology, Camino a la Presa San José 2055, San Luis Potosí S.L.P, CP 78216, Mexico.
E-mail address: noelc@ipicyt.edu.mx (N. Carbajal).
Peer review under the responsibility of the Institute of Oceanology of the Polish Academy of Sciences.

Production and hosting by Elsevier

https://doi.org/10.1016/j.oceano.2021.03.002

1. Introduction

In the Colorado River's Delta, an extraordinary phenomenon of resuspension and sediment deposition occurs in the neap-spring cycle of tidal currents. A detailed analysis of a collection of satellite images revealed the presence of Kelvin-Helmholtz (K-H) instabilities at different locations in the delta. The resuspension of sediment occurs in filaments, which makes the instabilities of Kelvin-Helmholtz visible. The discovery of K-H instabilities in the delta made it possible to string together a series of physical and dynamic conditions that finally explained the phenomenon. This investigation implied reviewing the conditions in which K-H instabilities occur, such as velocity shears, topography, and properties of tidal flows, to explain the wavelengths observed in satellite images theoretically. Kelvin-Helmholtz instabilities are a common but not always visible phenomenon. A brief description of the K-H instabilities observed in different situations follows.

Velocity shear between fluid layers leads to disturbances that manifest as a kind of Kelvin-Helmholtz instabilities. The fluid layers are mostly parallel fluid streams with different speeds and often with different densities. In the turbulence initiation, the velocity shear in the ocean or the atmosphere and a density difference between two flow bands are necessary conditions to explain initial instabilities in their most comprehensive form. Theoretical considerations, laboratory experiments (Thorpe, 1971), and observations in the atmosphere suggest that a form of dynamic instability commonly referred to as K-H instability triggers air turbulence. The variety of situations and places where the K-H instabilities occur gives it practically a universal character. K-H instabilities at the interface of flow layers often occur in the ocean and the atmosphere and astronomical bodies like in comet tails or on Saturn and Jupiter's Surface (Ershkovich, 1980; Masters et al., 2009). These instabilities frequently occur in the Earth's atmosphere, where they are a common phenomenon. At the interface of a temperature inversion, acoustic measurements of the lower atmosphere have revealed patterns that resemble K-H instabilities (Emmanuel et al., 1972). Remote sensing measurements and in situ observations, coupled with a numerical simulation, were used to understand the dynamic instability of Peru's upper troposphere. A large-scale shear in the upper troposphere became locally unstable to ambient gravity wave activity. It allowed gaining an insight into isolated K-H instabilities events that grew to develop a large mixing layer (Kelley et al., 2005). Instability due to velocity shear plays a significant role in mixing processes in stratified fluids in the atmosphere and the ocean. Perhaps the visualization of K-H instabilities is more difficult in the ocean where the phenomenon seems to appear less frequently, but there is evidence that it often occurs even in the deep ocean (Hua and Hidekatsu, 2001; van Haren and Gostiaux, 2010). Velocity shear in rivers and estuaries also exhibit K-H instabilities. The turbulence generated in this process can occur at moderate values of the Reynolds number, in which the rupture of the stratified density structure can happen. Using backscatter profiles and in situ measurements of velocity, temperature, and conductivity, it was possible to generate echo-sounding images of inner and outer transects within the K-H instabilities waves (Geyer et al., 2010). Their measurements, carried out in a river, revealed that turbulence occurred not in the instability core but within secondary shear instabilities areas of intensified shear around the core for a very high Reynolds number. These instabilities are smaller and are called secondary instabilities of the K-H type. Geyer and Smith (1987) found that shear instability is the principal mechanism of vertical exchange within the salt wedge estuary's pycnocline. Although several modes describe the instability process, the fastest instability growth mode under typical conditions of stratification and flow shear is the one that best explains the type of K-H instabilities (Hazel, 1972). Evidence now exists that unstable velocity shears in the atmosphere and the ocean can excite various wave disturbances. These disturbances range from modes trapped at the unstable velocity shear to modes that may propagate away in one or both directions. Several Researchers studied the trapped mode, or K-H instability, which is the source of much atmospheric and oceanic turbulence (Fritts, 1979). De Silva et al. (1996) present an extensive discussion on K-H instabilities in the atmosphere, ocean, and laboratory experiments. They found that small-scale turbulent mixing is present within billows from the early stages of their evolution. However, when the billows achieve maximum height, mixing becomes intense, and the billows decay.

In order to explain K-H instabilities in the Colorado River Delta, two fundamental aspects must be highlighted: firstly, the tidal signal undergoes robust amplification that is reflected in intense tidal currents, and secondly, in geological times, the Colorado River deposited enormous amounts of sediment much of which is still found in the delta. The result is strong sediment mobility caused by currents modulated by the dominant tidal components. The tides in the delta have a semi-diurnal character. The most important being the principal lunar tide M2 and the principal solar tide S2. These two tidal components interact constructively and destructively over 14.7 days. When the interaction is destructive in a neap tidal situation, the tidal currents are small; as the interaction becomes constructive, the currents intensify, initiating a very intense sediment resuspension process in the delta. When the tides reach the maximum of constructive interaction, i.e., at spring tides, the currents are powerful with speeds up to 3 m s^{-1}. In this situation, the suspended sediment occupies the delta completely. An essential characteristic of this extraordinary sediment dynamic is that the resuspension of sediments begins in the form of filaments in such a way that there is a finger-like pattern (Carbajal et al., 2020). A detailed analysis of satellite images revealed that these filaments make K-H instabilities visible at some points. This work's primary purpose is to understand why these instabilities occur and explain the factors that combine for the phenomenon's occurrence.

2. The Colorado River Delta

The Colorado River Delta is a region that has suffered from anthropogenic actions like dams and irrigation systems for agriculture upstream of the river. With its triangular shape, the delta received a discharge of water that could exceed 2000 m^3 s^{-1}. In geological times, a massive discharge of sediments occurred so that today dominates the seabed of

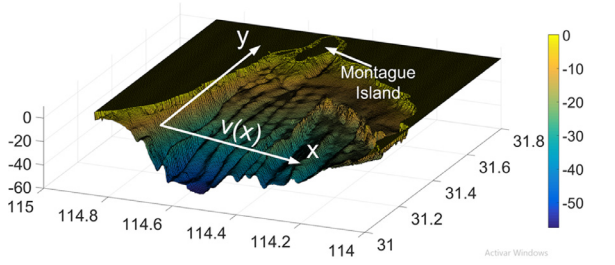

Figure 1 Bathymetry of the Colorado River Delta. The coordinate system applied in the theory is also indicated. $v(x)$ represents the y-component of the velocity vector, while its variability occurs on the x-axis.

the delta. With the construction of dams, the delta dynamics changed from estuarine to that of the reverse estuary. Today, intense tidal currents, impressive sediment mobility, and undulating topography (Figure 1) characterize the delta. The observed sea-level amplitudes at the tidal signal passage can reach a tidal range of more than 10 m with speeds of up to 3 m s^{-1} in some narrow points of the delta and in areas where the flow is channeled (Carbajal, 1993). This channeling process can be explained by the delta seabed morphology, which shows an undulating topography with a series of ridges and troughs that extend approximately 60 km to the south. This undulating form results from the interaction of tidal currents with the seabed sediment; it arises due to morphological instabilities of the seafloor Carbajal and Montaño, 2001; Hulscher, 1996). In this process of instability, sandbanks represent areas of accumulation of sediment and troughs areas of erosion. The interaction between tidal currents and the seabed is a continuous process. Assuming that the system reached a steady state, then the flow towards the sandbanks is compensated by the sediment that, through diffusion processes, is deposited in the troughs (Zhu and Chang, 2000). Off (1963) described similar bedforms in the North Sea as tidal current ridges. The same regular pattern receives several names in the available literature: linear sandbanks (Huthnance, 1982; Hulscher, 1996) and ridges (Pattiaratchi and Collins, 1987). Linear sandbanks are quasi-periodic bedforms roughly aligned with tidal currents and occurring widely on continental shelf areas. Sufficient sand availability and strong enough hydrodynamic processes are necessary to transport the sediment and generate sandbanks. Sedimentation in the Colorado River Delta and the upper Gulf of California, including sandbanks, has been studied by Carriquiry and Sánchez (1999). Montaño and Carbajal (2008) investigated the instability process in the interaction of tidal currents with the seabed that leads to the formation of sandbanks in the Colorado River Delta.

The dominant semidiurnal tides, M_2 and S_2, with their constructive (spring tides) and destructive (neap tides) interaction of approximately 14.7 days, cause extraordinary mobility of sediments captured by satellite images throughout the process. The satellite images clearly show the initial resuspension process, which begins on the delta's north side (Figure 2). Resuspension begins on the sandbanks' ridges, where friction is more vigorous (Carbajal et al., 2020). The satellite images reveal how little by little the sediment filaments extend towards the south, and simultaneously a lateral diffusion process occurs due to turbulence. During the spring tides period, the sediment has diffused throughout the delta, and there is a more homogeneous sediment concentration (Figure 3). As the dynamics move towards the neap tides, the velocities decrease, and the sediment begins to settle until it is almost wholly deposited, and the

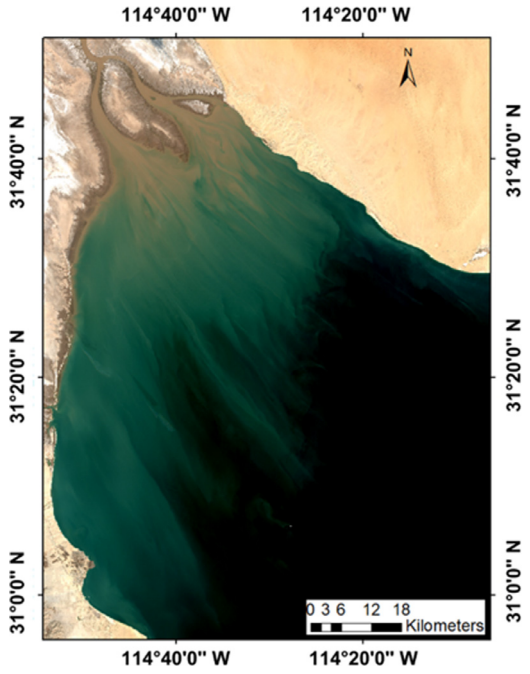

Figure 2 Resuspension process a few days after neap tides. The finger–like pattern arises because the sediment is suspended above the ridges of the undulating bathymetry.

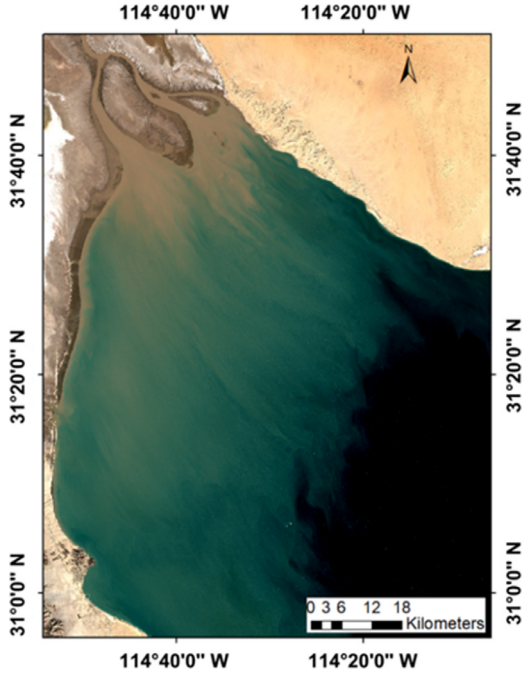

Figure 3 Suspended sediment distribution during spring tides. The sediment is dispersed practically throughout the delta.

14.7-day cycle begins again. We use data acquired by Sentinel-2B in April 2017 (Figure 2) and November 2017 (Figure 3). The images were downloaded from the Copernicus Open Access Hub website (https://scihub.copernicus.eu/). Atmospheric correction was done using the Sentinel Application Platform (SNAP) software using a plugin called Sen2Cor (v.2.4.0). In both figures, a composition of NIR, Red, and Green bands (8, 4, 3) was used to enhance the phenomenon further.

Although the image shown in Figure 3 shows a practically homogeneous distribution of suspended sediment throughout the delta, it has been found in grain size measurements that on the east side of the delta, the grain size varies between 63 and 500 μm and on the west between 3 and 63 μm (Carriquiry and Sánchez, 1999). It is important to note that observed concentrations reveal an inhomogeneity. Álvarez and Jones (2002) found different situations and at different points of the delta values between 3 and 35 mg l^{-1}, with maximum values higher than 100 mg l^{-1}. The phenomenon of resuspension and sediment deposition caused by the variability of tidal currents in the neap-spring tidal cycle is an extraordinary sedimentary phenomenon. Nevertheless, this process hides an additional phenomenon that only a detailed analysis of satellite images reveals, i.e., the phenomenon of K-H instabilities in the Colorado River Delta. The physical and dynamic conditions and the presence of suspended sediment suggest an explanation for the occurrence and visualization of this phenomenon of Kelvin-Helmholtz instability.

3. Instability of Kelvin-Helmholtz

Several factors intervene in the generation of K-H instabilities in the delta: First, the tides' manifestation is notable, with ranges of approximately 10 m in spring tides that produce intense currents in the ebb and flood stages. Second, the delta has a high sediment availability. Third, the topography is undulating across the delta. The series of ridges and troughs produce a variability of tidal currents across the delta, causing velocity shears with stronger velocities on sandbanks' ridges than in the troughs. The dominant tides are the semidiurnal M2 and S2. The constructive and destructive interaction of the M2 and S2 tides occurs in a cycle of about 14.7 days. At neap tides, the dynamics decay with the sediment almost entirely settled on the seabed. In this period, satellite imagery reveals very little suspended sediment. As the tidal dynamics go from neap to spring tides, the currents intensify until reaching a threshold velocity with which the resuspension process begins. This process begins in the neighborhood of Montague Island and later extends southwards. Satellite imagery reveals that the resuspension process occurs in the form of filaments with a finger-like pattern (Figure 4). Furthermore, the sediment resuspension process occurs on the sandbanks' ridges and subsequently extends through lateral diffusion until it homogeneously occupies the entire delta (Carbajal et al., 2020) (Figure 3). When the tidal currents decrease in intensity and approach a neap tidal situation, the sediment is deposited, which ends.

The satellite image shown in Figure 4 reveals the remarkable K-H instabilities manifesting as disturbances with

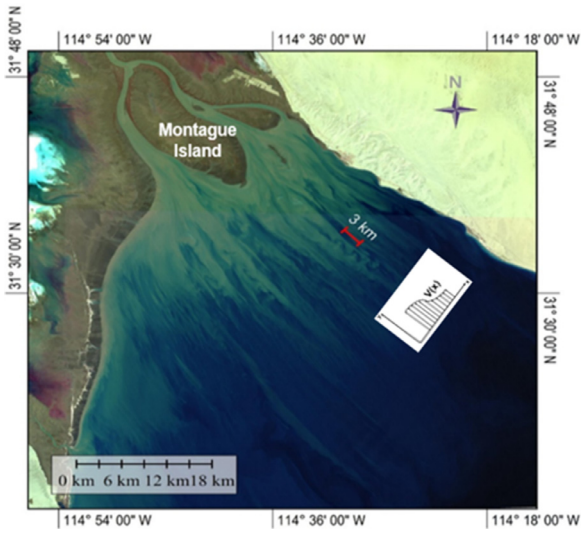

Figure 4 Distribution of suspended sediment in the form of filaments in time close to neap tides. The image also shows the K-H instability with a wavelength of approximately 3 km and the velocity shear proposed in the theory is observed.

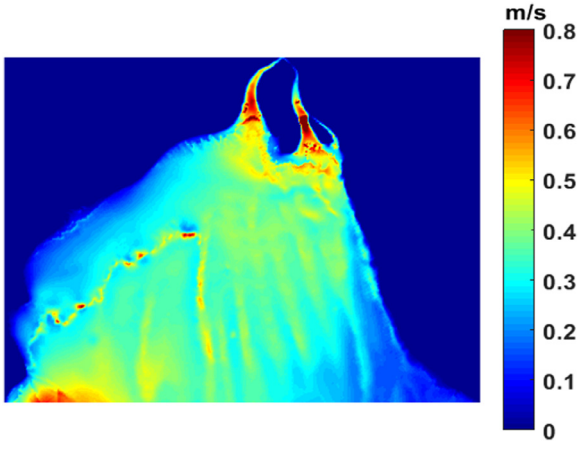

Figure 5 Distribution of the instantaneous absolute value of the velocity vector in the Colorado River Delta, during flood tides, near spring tides.

a wavelength of approximately 3 km. The image was taken on September 10, 2018, at 6:15:53 PM UTC, and it depicts the process of sediment resuspension a few days after spring tides when suspended sediment has already been deposited partially in the deeper southern part. The image reveals a different degree of resuspension, with more suspended sediment in the north side's shallower parts. It suggests that resuspension is a function of depth or, more directly, of friction. When comparing Figure 1 and Figure 4 and using the geographic information system (GIS), it is possible to verify that the filaments occur on the delta sandbank system's ridges. The abundance of filaments and the number of sandbanks in the undulating topography suggest that K-H instabilities occur at various Colorado River Delta locations.

It is necessary to investigate the velocity shears present in the tidal currents that occur in the delta due to the bathymetry's undulating shape to explain K-H instabilities. Figure 5 shows the instantaneous absolute value of

the velocity vector calculated in a numerical simulation with a vertically integrated two-dimensional model. The simulation considered the tidal constituents M2 and S2. Figure 5 corresponds to a flood situation near spring tides. Surprisingly, the speed distribution resembles the suspended sediment finger-like pattern. On the sandbanks' ridges, the water's speed is around 0.08–0.15 m s^{-1} higher than in the troughs, i.e., there is a velocity shear between the crest and troughs, which occurs in large areas of the delta. Comparing the distribution of the speed of tidal currents (Figure 5) with the satellite image of the filaments (Figure 4) reveals a remarkable coincidence between higher speed values over ridges and the suspended sediment filaments. Since K-H instabilities occur in velocity shears, the analysis suggests that the instabilities, shown in Figure 4, must occur somewhere between the ridges and troughs of the undulating topography. It is reasonable to think that in other parts of the world where there are sandbanks, velocity shears and K-H instabilities can occur. There are many places where tidal currents are intense, and sediment availability is enough to form sandbanks due to the well-known process of instability caused by the interaction between tidal currents and sediment. It would be interesting to investigate whether K-H instabilities occur in places like the North Sea, the Gulf of Korea, the Gulf of Khambhat, Jiangsu coast in China, the Persian Gulf, Moreton Bay in Australia, among other regions.

The above analysis suggests that K-H instabilities occur in velocity shears induced by undulating topography. A search for K-H instabilities on satellite imagery revealed that such instabilities exist in various Colorado River Delta locations. Figure 6 shows two different places in the delta where instabilities occur: Figure 6a (March 4, 2018, at 18:17:20 UTC) displays instabilities at the coordinates 30°32′00″N and 114°26′00″W with wavelengths of about 1.8 km. Figure 6b (July 5, 2019, at 18:35:43 UTC) shows instabilities approximately at the coordinates 31°37′30″N and 114°41′00′'W with wavelengths of about 1.8 km. Figure 4 (September 10, 2018, at 18:15:53 UTC) shows instabilities approximately at the coordinates 31°33′00″N and 114°29′00″W with wavelengths of about 3.0 km. The order of magnitude of the wavelengths is quite similar in all three cases, suggesting that the velocity shear is of the same order causing a similar instability strength. A possible explanation is that the tidal phenomenon is practically the same, i.e., the sea elevation gradients generate currents of the same order throughout the delta.

It is important to note that the shown cases of K-H instabilities are not arbitrarily selected phenomena. There are high-resolution satellite images for this area of the Gulf of California since 2016. The instability phenomenon occurs at a given time in the 14.7-day cycle from neap to spring tides, and the Sentinel satellite crosses the area approximately every four days. The probability of capturing the phenomenon of K-H instabilities reduces drastically. Despite these limitations, it was possible to find a remarkable satellite image, acquired on March 13, 2020, where the generation of K-H instabilities is observed practically along all the sandbanks (Figure 7). The instabilities coincide with the sandbanks' position shown in Figure 1 or with absolute values of the velocity in the finger-like form shown in Figure 5. This fact strengthens the hypothesis that sandbanks favor the existence of velocity shears, which generates K-H insta-

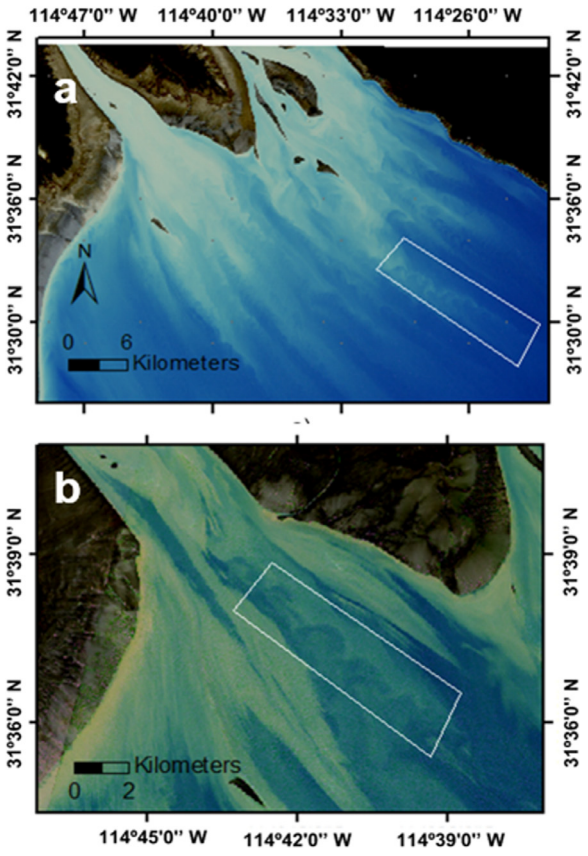

Figure 6 Examples of wave formation in the Colorado River Delta acquired by Sentinel 2 satellite data: a) scene acquisition data: March 4, 2018, wavelength: 1.8 km, time of acquisition: 18:17:20 UTC and b) scene acquisition data: July 5, 2019, wavelength: 1.8 km, time of acquisition: 18:35:43 UTC.

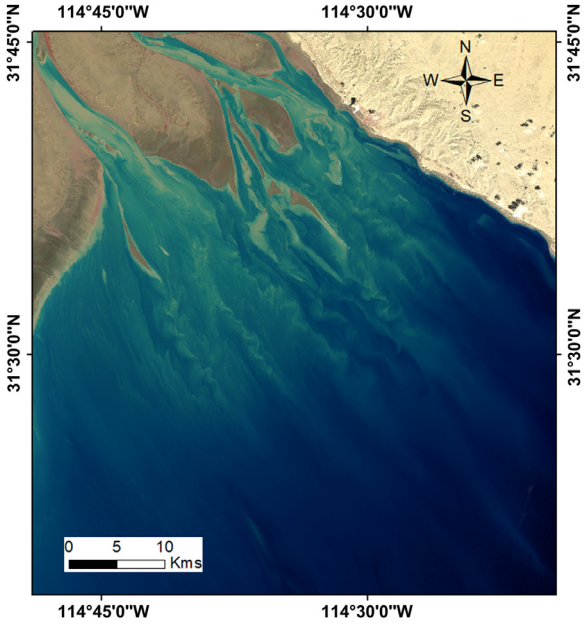

Figure 7 Satellite image showing the generation of Kelvin-Helmholtz instabilities in practically the entire Colorado River Delta. Acquired by Sentinel 2 satellite data: March 13, 2020, time of acquisition 18:25:37 UTC.

bilities. The wavelengths fall in the range of those discussed in Figures 4, 6a, and 6b.

4. Theory

The purpose of this first part of the theory is to explain the shape of the velocity shears in the transition zone of two flows with different speeds that produce disturbances that can grow and become shear instabilities (or K-H instabilities). Figure 5 shows the absolute value of the velocity vector where faster areas can be distinguished on sandbar ridges than in troughs with velocity differences of about 0.1 $m\,s^{-1}$. This fact justifies a closer look at the horizontal shear in the Colorado River Delta. Great scientists like Helmholtz and Kelvin established the mathematical foundations to explain instabilities in velocity shears, as well as renowned scientists of the 20th century took up the subject. About the topic, Markowski and Richardson (2010) describe how to deal with shear instabilities mathematically. Considering a flux oriented south-north (y) and varying in the west-east direction (x) (see coordinate system in Figure 1), consider the velocity in the y-direction, $v = \bar{v} + v'$, with $\bar{v} = \bar{v}(x)$, where the perturbation is in the x-y plane. The velocity in the x direction is given by $u = \bar{u} + u'$, with $\bar{u} = 0$, that is, in the x direction there is no average flow. For the south-north velocity, v, the following geostrophic balance is assumed, $\bar{v} = (1/f)\partial_x\bar{\phi}$ where the hydrostatic equation and the geopotential, $\emptyset = \bar{\emptyset} + \emptyset'$, with $\bar{\emptyset} = \bar{\emptyset}(x)$, have been used. In addition, the vorticity equation was applied in the form, $\partial_t\zeta + u\partial_x\zeta + v\partial_y\zeta + \beta v = 0$. With the linear coefficient of variation in the beta plane, $\beta = d_x f$, and $\zeta = \partial_x v - \partial_y u$ is the vertical component of the vorticity. Substituting in the variables of the vorticity equation the sum of an averaged, and a perturbed part, $u = \bar{u} + u', v = \bar{v} + v'$, $\zeta = \bar{\zeta} + \zeta'$, and assuming that the average variables satisfy the form of the original vorticity equation, results $\partial_t\zeta' + \bar{v}\partial_y\zeta' + \bar{u}\partial_x\zeta' + u'\partial_x\bar{\zeta} + v'\partial_y\bar{\zeta} + \beta v' = 0$. Applying the equalities, $\bar{\zeta} = \partial_x\bar{v} - \partial_y\bar{u} = \partial_x\bar{v}$, $\zeta' = \partial_x v' - \partial_y u' = (1/f)(\partial^2_{x^2} + \partial^2_{y^2})\phi'$, $u' = -(1/f)\partial_y\phi'$ and $v' = (1/f)\partial_x\phi'$, the following equation is obtained

$$\left(\frac{\partial}{\partial t} + \bar{v}\frac{\partial}{\partial y}\right)\left(\frac{\partial^2}{\partial x^2} + \frac{\partial^2}{\partial y^2}\right)\emptyset' - \frac{\partial\emptyset'}{\partial y}\frac{\partial^2\bar{v}}{\partial x^2} + \frac{\partial\emptyset'}{\partial x}\frac{\partial^2\bar{v}}{\partial x\partial y} + \beta\frac{\partial\emptyset'}{\partial x} = 0 \tag{1}$$

Considering an oscillatory movement of the form, $\emptyset' = \hat{\emptyset}(x)e^{ik(y-ct)}$, assuming that $\hat{\emptyset}(x)$, and the phase velocity c are complex, i.e. $\hat{\emptyset} = \hat{\emptyset}_r + i\hat{\emptyset}_i$, $c = c_r + ic_i$, with the conjugate complex, $\hat{\emptyset}^* = \hat{\emptyset}_r - i\hat{\emptyset}_i$, and $c^* = c_r - ic_i$, multiplying the equation by the conjugate complex, with the approximation $\beta = d_x f$=0, and integrating the equation in the x direction from −L to L (integrating by parts), the following equation is obtained

$$\int_{-L}^{L}\left(\left|\frac{d\hat{\emptyset}}{dx}\right|^2 + k^2\left|\hat{\emptyset}\right|^2\right)dx + a\int_{-L}^{L}\frac{\frac{\partial^2\bar{v}}{\partial x^2}\left|\hat{\emptyset}\right|^2}{(a^2 + c_i^2)}dx + ic_i\int_{-L}^{L}\frac{\frac{\partial^2\bar{v}}{\partial x^2}\left|\hat{\emptyset}\right|^2}{(a^2 + c_i^2)}dx = 0 \tag{2}$$

where a is a variable defined by $a = \bar{v} - c_r$. The Equation (2) is equal to zero and contains a real part and an imaginary part, i.e., each part must be independently equal zero. Except for the term, $\partial^2_{x^2}\bar{v}$, all elements of Equation (2) are squared and positive. The only way that the term of the complex part is equal to zero is that $\partial^2_{x^2}\bar{v} = 0$. From differential calculus, when the second derivate of a function is zero, it implies that there should be an inflection point where the curve changes from concave to convex or vice versa. Since the tides move in the same direction at a given time, there can be no velocities in opposite directions to explain the inflection point. The variation of the velocity $v(x)$ should be as shown in Figure 4, with higher speeds on the ridges and lower in the troughs, and a curve with an inflection point. The interaction of the oscillating tidal flow with the undulating topography produces a velocity shear with the condition, $\partial^2_{x^2}\bar{v} = 0$. According to Figure 7, this condition is satisfied in all the sandbanks of the Colorado River Delta. It is interesting to explore in other seas where there are sandbanks caused by tidal flows if K-H instabilities occur.

The theoretical relationship between wavelength of a K-H instability and the velocity difference between the layers is investigated. Consider a predominantly one-dimensional incompressible flow in the y-direction as the longitudinal axis, and the x-direction as the transverse axis. Following Landau and Lifshitz (1987), the contact surface at $x = 0$ has a tangential velocity discontinuity of the form: $\bar{v}_1(x > 0, y) = [0, v_1]$, and $\bar{v}_2(x < 0, y) = [0, v_2]$. The perturbations $\bar{v}'_k = [u'_k, v'_k]$ with $k = 1, 2$ corresponding to each layer, satisfy the continuity equation $\bar{\nabla}\circ\hat{v}'_k = \partial_x u'_k + \partial_y v'_k = 0$ and the motion equation $\partial_t\bar{v}'_k + (v_k\partial_y)\bar{v}'_k = -(1/\rho_k)\bar{\nabla}p'_k$ (ρ_k stands for density and p_k for pressure). Applying the divergence, the equation, $\bar{\nabla}\circ\bar{\nabla}p_k = (\partial^2_x + \partial^2_y)p'_k = 0$, is obtained. Progressive waves in the y direction with the amplitude depending on x are considered, the perturbed pressure is given by $p'_k = p'_{0k}(x)e^{i(ky-\omega t)}$. The solutions for each layer are $p'_1(x > 0, y) = c_0\,e^{-kx}e^{i(ky-\omega t)}$ and $p'_2(x < 0, y) = c_1\,e^{kx}e^{i(ky-\omega t)}$, where c_0 and c_1 are constants, this would be the shape that the perturbations of the other variables would acquire. In a frame of reference at rest with the second layer, the first one have the velocity, $\Delta v = v_1 - v_2$. Substituting the solutions proposed above in the equation of motion of each layer, considering that at the tangential contact surface between the layers the pressures p'_1 and p'_2 are equal and the introduction of a displacement function perpendicular to the contact surface due to the disturbance can be demonstrated that the following equation for the relation between $\omega = 2\pi/T$ and $k = 2\pi/\lambda$ is obtained.

$$\omega = k\,|\Delta u|\{1 \pm i\rho_{21}^{1/2}\}/(1 + \rho_{21})\,(\rho_{21} = \rho_2/\rho_1) \tag{3}$$

The form of the imaginary part indicate that there will always be amplification of instabilities. The real part leads to $\lambda = T\,|\Delta u|/\,(1 + \rho_{21})$, and in the case of layers of the same fluid to

$$\lambda = \tfrac{1}{2}T\,|\Delta u| \tag{4}$$

In the Colorado River Delta, the predominant tides are the semidiurnal M2 ($T_{M2} = 12.42h$) and S2 ($T_{S2} = 12h$). According to Figures 4, 6a and 6b, the disturbances wavelengths are $\lambda \to$ [3.0, 1.8, 1.8] km, then the speed differences that originate them should be of the order of

$\Delta u \rightarrow$ [0.13, 0.08, 0.08] m s^{-1}, which is in close agreement with the calculated speed differences shown in Figure 5 of around 0.08—0.15 m s^{-1}.

According to the satellite images shown in Figures 4, 6, and 7, the K-H instabilities occur along the sandbanks in the Colorado River Delta. They arise from velocity shears in the tidal flow that are caused by the undulating topography. The resuspension of sediment in the form of filaments makes these K-H instabilities visible. For the occurrence of K-H instabilities, the theory predicts that the velocity shears must have an inflection point. This inflection point can be caused in the delta by undulating topography. Based on the theory and using the wavelengths of the observed instabilities, the velocity shears that produce them were estimated. The observed and predicted velocity shears coincide quite well.

5. Conclusions

The occurrence of K-H instabilities in the Colorado River Delta has been described and explained through a series of collected satellite images reflecting K-H instabilities in the delta area. Intense semidiurnal tidal currents, undulating topography due to existing sandbanks, and an enormous sediment availability that is suspended and deposited in a 14.7-day cycle combine to cause and visualize K-H instabilities. Suspended sediment makes visible the K-H instabilities, which are captured in satellite images. The ridges and troughs extending longitudinally in the delta cause flow variation, with higher speeds over the ridges than the troughs. It is this velocity shear that produces the K-H instabilities, which are captured in satellite images and the suspended sediment did make them visible. The different wavelengths observed in satellite images and the periods of semidiurnal tides made it possible to calculate the velocity shear that should have occurred. These velocity shears predicted by Equation (4) coincide with those modeled numerically. The theory correctly predicts the observed wavelengths. The requirement of a velocity shear with an inflection point is explained in the delta by the sandbanks' presence. Figure 7 demonstrates that K-H instabilities are possible along practically all sandbanks in the delta.

Declaration of Competing Interest

The authors declare that they have no known competing financial interests or personal relationships that could have appeared to influence the work reported in this paper.

References

Álvarez, L.G., Jones, S.E., 2002. Factors influencing suspended sediment flux in the upper Gulf of California. Estuar. Coast. Shelf. Sci. 54, 747—759. https://doi.org/10.1006/ecss.2001.0873

Carbajal, N., 1993. Modelling of the circulation of the Gulf of California, Berichte aus dem Zentrum für Klima- und Meeresforschung. Reihe B, Nr. 3.

Carbajal, N., Montaño, Y., 2001. Comparison between predicted and observed physical features of sandbanks. Estuar. Coast. Shelf Sci. 52, 435—443. https://doi.org/10.1006/ecss.2000.0760

Carbajal, N., Montaño-Ley, Y., Soto-Jiménez, M., Páez-Osuna, F., Tuxpan, J., 2020. Finger-like plumes of suspended sediment in the Colorado River Delta, Gulf of California. Estuar. Coast. Shelf Sci. 245, 106996. https://doi.org/10.1016/j.ecss.2020.106996

Carriquiry, J.D., Sánchez, A., 1999. Sedimentation in the Colorado River delta and the upper Gulf of California after nearly a century of discharge loss. Mar. Geol. 158, 125—145. https://doi.org/10.1016/S0025-3227(98)00189-3

De Silva, I.P.D., Fernando, H.J.S., Eaton, F., Hebert, D., 1996. Evolution of Kelvin-Helmholtz billows in nature and laboratory. Earth Planet. Sci. Lett. 143, 217—231. https://doi.org/10.1016/0012-821X(96)00129-X

Emmanuel, C.B., Bean, B.R., McAllister, L.G., Pollard, J.R., 1972. Observations of Helmholtz waves in the lower atmosphere with an acoustic sounder. J. Atmos. Sci. 29, 886—892. https://doi.org/10.1175/1520-0469(1972)029⟨0886:OOHWIT⟩2.0.CO;2

Ershkovich, A.I., 1980. Kelvin-Helmholtz instability in type-1 comet tails and associated phenomena. Space Sci. Rev. 25, 3—34. https://doi.org/10.1007/BF00200796

Fritts, D.C., 1979. The excitation of radiating waves and Kelvin-Helmholtz instabilities by the gravity wave-critical level interaction. J. Atmos. Sci. 36, 12—23. https://doi.org/10.1175/1520-0469(1979)036⟨0012:TEORWA⟩2.0.CO;2

Geyer, W.R., Lavery, A.C., Scully, M.E., Trowbridge, J.H., 2010. Mixing by shear instability at high Reynolds number. Geophys. Res. Lett. 37 (22). https://doi.org/10.1029/2010GL045272

Geyer, W.R., Smith, J.D., 1987. Shear instability in a high stratified Estuary. J. Phys. Ocean. 17, 1668—1679. https://doi.org/10.1175/1520-0485(1987)017⟨1668:SIIAHS⟩2.0.CO;2

Hazel, P., 1972. Numerical studies of the stability of inviscid stratified shear flows. J. Fluid Mech. 51 (1), 39—61. https://doi.org/10.1017/S0022112072001065

Hua, L., Hidekatsu, Y., 2001. Observations of a Kelvin-Helmholtz billow in the ocean. J. Ocean. 57, 709—721. https://doi.org/10.1023/A:1021284409498

Hulscher, S.J.M.H., 1996. Formation and migration of large scale, rhythmic seabed patterns. Univ. Utrecht, Holland, 143 pp.

Huthnance, J., 1982. On one mechanism forming linear sandbanks. Est. Coast. Shelf Sci. 14, 79—99. https://doi.org/10.1016/S0302-3524(82)80068-6

Kelley, M.C., Chen, C.Y., Beland, R.R., Woodman, R., Chau, J.L., Werne, J., 2005. Persistence of a Kelvin-Helmholtz instability complex in the upper troposphere. J. Geophys. Res. 110 (D14). https://doi.org/10.1029/2004JD005345

Landau, L.D., Lifshitz, E.M., 1987. Course of Theoretical Physics, 2 edn., Fluid Mech., Vol. 6, Pergamon Press.

Markowski, P., Richardson, Y., 2010. Mesoscale meteorology in midlatitudes. Wiley-Blackwell, 407 pp.

Masters, A., Achilleos, N., Bertucci, C., Dougherty, M.K., Kanani, S.J., Arridge, C.S., McAndrews, H.J., Coates, A.J., 2009. Surface waves on Saturn's dawn flank magnetopause driven by the Kelvin—Helmholtz instability. Planet. Space Sci. 57 (14—15), 1769—1778. https://doi.org/10.1016/j.pss.2009.02.010

Montaño, Y., Carbajal, N., 2008. Numerical experiments on the long-term morphodynamics of the Colorado River Delta. Ocean Dyn. 58, 19—29. https://doi.org/10.1007/s10236-007-0129-y

Off, T., 1963. Rhythmic linear sand bodies caused by tidal currents. Bull. Am. Ass. Petroleum Geol. 47, 324—341. https://doi.org/10.1306/BC743989-16BE-11D7-8645000102C1865D

Pattiaratchi, C., Collins, M., 1987. Mechanisms for linear sand bank formation and maintenance in relation to dynamical oceanographic observations. Prog. Oceanogr. 19, 117—156. https://doi.org/10.1016/0079-6611(87)90006-1

Thorpe, S.A., 1971. Experiments on the instability and turbulence in a stratified shear flow. J. Fluid Mech. 46, 299—319. https://doi.org/10.1017/S0022112073000911

Van Haren, H., Gostiaux, L., 2010. Gostiaux A deep-ocean Kelvin-Helmholtz billow train. Geophys. Res. Lett. 37 (3). https://doi.org/10.1029/2009GL041890

Zhu, Y., Chang, R., 2000. Preliminary study of the dynamic origin of the distribution pattern of bottom sediments on the continental shelves of the Bonhai Sea, Yellow Sea and East China Sea. Estuar. Coast. Shelf Sci. 51, 663—680. https://doi.org/10.1006/ecss.2000.0696